ARCHIVIO ISTITUZIONALE
DELLA RICERCA

Alma Mater Studiorum Università di Bologna
Archivio istituzionale della ricerca

Lactate dehydrogenase inhibition affects homologous recombination repair independently of cell metabolic asset; implications for anticancer treatment

This is the final peer-reviewed author's accepted manuscript (postprint) of the following publication:

Published Version:
Balboni, A., Govoni, M., Rossi, V., Roberti, M., Cavalli, A., Di Stefano, G., et al. (2021). Lactate dehydrogenase inhibition affects homologous recombination repair independently of cell metabolic asset; implications for anticancer treatment. BIOCHIMICA ET BIOPHYSICA ACTA-GENERAL SUBJECTS, 1865(1), 1-10 [10.1016/j.bbagen.2020.129760].

Availability:
This version is available at: https://hdl.handle.net/11585/781224 since: 2020-11-18

Published:

DOI: http://doi.org/10.1016/j.bbagen.2020.129760

Terms of use:

Some rights reserved. The terms and conditions for the reuse of this version of the manuscript are specified in the publishing policy. For all terms of use and more information see the publisher's website.

This item was downloaded from IRIS Università di Bologna (https://cris.unibo.it/).
When citing, please refer to the published version.

(Article begins on next page)

16 September 2026

Lactate dehydrogenase inhibition affects homologous recombination repair independently of cell metabolic asset; implications for anticancer treatment.

Andrea Balboni[a*], Marzia Govoni[b*], Valentina Rossi[b], Marinella Roberti[c], Andrea Cavalli[a,c], Giuseppina Di Stefano[b#] and Marcella Manerba[a,b]

a) Computational & Chemical Biology, Istituto Italiano di Tecnologia, via Morego 30, 16163 Genova, Italy.
b) Department of Experimental, Diagnostic and Specialty Medicine, University of Bologna, Via San Giacomo 14, 40126 Bologna, Italy.
c) Department of Pharmacy and Biotechnology, University of Bologna, Via Belmeloro 6, 40126 Bologna, Italy.

* These Authors contributed equally

Corresponding Author

Prof. Giuseppina Di Stefano
Department of Experimental, Diagnostic and Specialty Medicine
University of Bologna, Via San Giacomo 14, 40126 Bologna, Italy.
Email: giuseppina.distefano@unibo.it

Abstract

Background: Cancer cells show highly increased glucose utilization which, among other cancer-essential functions, was found to facilitate DNA repair. Lactate dehydrogenase (LDH) activity is pivotal for supporting the high glycolytic flux of cancer cells; to our knowledge, a direct contribution of this enzyme in the control of DNA integrity was never investigated. In this paper, we looked into a possible LDH-mediated regulation of homologous recombination (HR) repair.

Methods: We identified two cancer cell lines with different assets in energy metabolism: either based on glycolytic ATP or on oxidative reactions. In cells with inhibited LDH, we assessed HR function by applying four different procedures.

Results: Our findings revealed an LDH-mediated control of HR, which was observed independently of cell metabolic asset. Since HR inhibition is known to make cancer cells responsive to PARP inhibitors, in both the cellular models we finally explored the effects of a combined inhibition of LDH and PARP.

Conclusions: The obtained results suggest for LDH a central role in cancer cell biology, not merely linked to the control of energy metabolism. The involvement of LDH in the DNA damage response could suggest new drug combinations to obtain improved antineoplastic effects.

General Significance: Several evidences have correlated the metabolic features of cancer cells with drug resistance and LDH inhibition has been repeatedly shown to increase the antineoplastic power of chemotherapeutics. By shedding light on the processes linking cell metabolism to the control of DNA integrity, our findings also give a mechanistic explanation to these data.

Keywords: Cancer cell metabolism; Glycolysis; Homologous recombination; Lactate; Lactate dehydrogenase; Olaparib

1. Introduction

Cancer can be essentially considered a metabolic disease, characterized by aberrant and/or dysregulated glucose metabolism and bioenergetics [1]. Neoplastic cells typically show highly increased rates of glucose uptake and glycolysis, after which the obtained pyruvate is converted to lactate by lactate dehydrogenase (LDH). In cells with defective mitochondrial function or residing in hypoxic tissue niches, lactate is usually extruded in the microenvironment; otherwise, this metabolite can be reconverted to pyruvate in mitochondria, providing additional energy fuel [2].

The highly increased glucose consumption observed in cancer cells is likely dictated by their continuous need of biosynthetic precursors, required to build up new macromolecules and to sustain the unrestricted cell proliferation. As well-known and just as an example, the sugar backbone of nucleotides is obtained from glucose-6-phosphate through the pentose phosphate pathway, which is also an essential source of NADPH, the “reducing power” driving anabolic processes [3].

The enhanced glucose metabolism was also found to promote other cancer-essential functions, such as metastatic spread [4], resistance to apoptosis [5] and genome stability [6]. Among these, the maintenance of a certain level of DNA integrity is a crucial function for supporting active proliferation, even for cancer cells already bearing genetic mutations. Interestingly, elevation of glycolysis was found to facilitate DNA repair and to confer cancer cells resistance to ionizing radiation [7]. Furthermore, considerable amounts of evidences suggest that inhibition of glycolysis leads to compromised DNA repair [8], which is accompanied by energy depletion. However, the mechanisms linking the glycolysis-based metabolic program to radiation resistance have not been fully understood, although alteration in pH and lactate levels have been implicated [9].

In the recent years, inhibition of the metabolic features of cancer cells began to be viewed as an attractive therapeutic option. In this context, LDH appears to be one of the most interesting potential targets for designing an anti-metabolic cancer treatment [10]. This enzyme is constantly overexpressed in cancer cells and, because of its position at the end of glycolytic pathway, it is considered not necessary for the viability of normal cells, which mainly catabolize pyruvate via the TCA cycle. Recently, the search of LDH inhibitors with drug-like properties has involved a number of pharmaceutical industries and research laboratories worldwide [11]. These efforts led to the identification of a number of small molecule inhibitors, which gave promising results in some preclinical settings and recently, a research team from the NCI announced the identification of a novel LDH inhibitor which was found to reduce tumor growth in vivo [12]. During these studies, impairment of energy metabolism obtained through LDH inhibition or downregulation was found to dampen some key features linked with the dysregulated cancer cell proliferation, such as the enhanced clonogenic potential and the metastatic spread [13,14]. Recent experiments addressing the function of LDH in cancer cell biology also evidenced for this enzyme a possible role beyond the mere management of pyruvate / lactate balance in glucose metabolism. In fact, similar to other glycolytic enzymes, LDH was found to be a protein “moonlighting” in cell nucleus [15], where it takes part in transcriptional complexes regulating gene expression [16]. In some experimental settings, the LDH-related antineoplastic effect was also found to be linked to LDH protein depletion rather than to glycolysis inhibition [14]. Furthermore, increasing evidences suggest for lactate a role as signaling factor, involved in the modulation of gene expression [9,17,18]. This metabolite was found to decrease chromatin compactness and enhance gene expression, an effect linked to histone hyperacetylation [17]. In some contexts, the increased gene expression was also found to be mediated by

the stimulation of a membrane receptor (HCA1/Gpr81) caused by the released metabolite. As a result, enhanced DNA repair capacity was observed [18].

Based on the above exposed premises, the experiments reported in the present paper were aimed at exploring a possible direct role of LDH in the DNA damage response (DDR). Our attention was focused on homologous recombination (HR) repair, a critical pathway to restore with high fidelity non-replication-associated double strand breaks (DSBs) and to mend collapsed replication forks. Intriguingly, cancer cells with defective HR show increased sensitivity to chemotherapeutic agents [19,20] and HR inhibition was suggested as a possible strategy to improve cancer cell response to therapy [21].

For these experiments we identified two human cancer cell models characterized by a different asset in energy metabolism: high reliance on glycolytic ATP production (BxPC-3 pancreatic adenocarcinoma) and, at the opposite, energy metabolism mainly based on oxidative reactions (SW620 colon adenocarcinoma). By using oxamate (OXA), a well-known LDH inhibitor with consolidated use [22], we tried to shed light on a possible LDH contribution in HR repair.

2. Materials and Methods

2.1 Cell cultures and treatments

BxPC3 and SW620 cells were grown in RPMI 1640 and DMEM medium, respectively. Both media were supplemented with 100 U/ml penicillin/streptomycin, 2 mM glutamine and 10% FBS. All the materials used for cell culture and reagents were obtained from Sigma-Aldrich, unless otherwise specified. Oxamate (OXA) and Olaparib (OLA, Selleckchem) were administered in culture medium. In OLA-including experiments, media were supplemented with 0.6% DMSO.

2.2 ATP and lactate levels

For ATP assay, 2 x 10^4 cells were plated in clear bottom 96-well white plates and treated for 3 h or 24 h with OXA. At the end of the treatment, ATP levels were measured by using the CellTiter-Glo Assay (Promega). Luminescence was assessed by using a Fluoroskan Ascent FL reader.

Lactate production was measured in OXA-exposed cells after 3h incubation at 37° in Krebs-Ringer medium. For both cultures, 5 x 10^5 cells were seeded in 6-well plates and treatments were performed in triplicate. The level of produced metabolite was assessed by using the method previously described [23].

2.3 Real-Time PCR

Cells were seeded in T25 flasks (7 x 10^5 cells / flask) and allowed to adhere overnight. Cultures were then exposed to OXA for additional 16 h. A 40 mM dose was used for SW620 cells; 20 mM for BxPC-3 cells. RNA was extracted using the PureZOL isolation reagent (Bio-Rad) and was quantified spectrophotometrically. Retro-transcription to cDNA was performed by using the Revert Aid™ First Strand cDNA Synthesis Kit, in different steps: 5 min denaturation at 65°C, 5 min annealing at 25°C, 1 h retro-transcription at 42°C and 5 min denaturation at 70°C. Real Time PCR analysis of cDNA (15 ng) was performed using SYBR Green (SSO Advanced, BioRad). The sequence of primers used for analyzing expression of the studied proteins and of the internal control genes are reported in Supplementary Information (Table S1).

For all examined genes, annealing temperature of primers was 60°C and the thermal cycler (CFX96 TM Real Time System, BioRad) was programmed as follows: 30 sec at 95°C; 40 cycles of 15 sec at 95°C; 30 sec at 60°C.

2.4 Plasmid recombination assay

Plasmid recombination was assessed by using a commercially available kit (Norgen). This assay is specifically designed to study bacterial recombination, but can be also applied

to mammalian cells. It is based on cell transfection with two plasmids that recombinate upon cell entry. The efficiency of recombination can be assessed by RT-PCR, using the primer mixtures included in the assay kit, which allow to discriminate between the original plasmid backbones and their recombination product.

Cells were seeded in a 24-well plate (2 x 10^5 cells/well, in duplicate) and treated with OXA for 16 h. Co-transfection with the two plasmids was performed in Lipofectamine 2000 (Invitrogen) for 5 h at 37°. During transfection cultures were also exposed to OXA. At the end of incubation, cells were washed with PBS and harvested; DNA was isolated using the QIAamp DNA mini kit (Qiagen). 25 ng of purified DNA was used for the real-time PCR, which was performed according to the protocol indicated by the manufacturer. Data analysis was based on the ΔΔCt method and compared the level of recombination assessed in OXA-exposed cells to that measured in control cultures.

2.5 Immunofluorescence of RAD51 in cell nuclei.

To visualize RAD51 in cell nuclei, BxPC-3 and SW620 cells were seeded on glass coverslips placed in a 6-well culture plate (2 x 10^5 cells/well) and allowed to adhere overnight. Cultures were then pre-incubated with OXA (20 and 40 mM for BxPC-3 and SW620 cells, respectively) for 16 h and subsequently exposed to 50 µM cisplatin for an additional 1.5 h. Medium was then removed and cultures were maintained in the presence of OXA for 5 h. After this time, cells growing on coverslips were fixed in PBS containing 1% paraformaldehyde for 20 min, permeabilized in 70% ethanol, air-dried and washed twice with PBS. Samples were incubated in 10% Bovine Serum Albumin (BSA) in PBS for 30 min at 37 °C and subsequently exposed to an anti-RAD51 rabbit polyclonal antibody (Bio Academia, 1:1000 in 5% BSA / PBS), overnight at 4 °C. After washing, coverslips were incubated with an anti-rabbit rhodamine-conjugated secondary antibody (Novus Biologicals;

1:600 and 1:1000 in 1% BSA / PBS, for BxPC-3 and SW620 cells, respectively) for 1 h at 37 °C, washed, air-dried, and mounted with a solution of DAPI (2µg/ml) and DABCO.

Images were acquired using a Nikon fluorescent microscope equipped with filters for rhodamine and DAPI. The percentage of cells bearing nuclear foci was estimated by two independent observers, by analyzing 100-250 cells for each treatment sample.

2.6 Neutral Red Viability Assay

Cells (1-2 x 10^4/well) were seeded in two 96-well plate. At the end of the treatment, cells were maintained in a medium containing 30 µg/ml Neutral Red for 3 h. Medium was then removed and the cells were solubilized with 200 µl of 1% acetic acid in 50% ethanol. The absorbance of the solutions was measured at λ540 using a microplate reader (Multiskan EX, ThermoLab Systems). To estimate cell numbers, before each experiment a plot reporting the Neutral Red absorbance values obtained from scalar amounts of cells was acquired for the used cell line.

In the experiments of OXA/OLA association, the combination index between the two compounds was calculated by applying the following procedure:

$$\frac{\text{Surviving cells treated with the OXA/OLA association}}{\text{(Surviving cells treated with OXA) x (Surviving cells treated with OLA)}}$$

2.7 Cytotoxicity Assay

Cell death was assessed by applying the CellTox™ Green Cytotoxicity Assay (Promega). Cells (1-2 x 10^4/well) were plated in clear-bottom 96-wells black plates. At the end of the treatment, the CellTox™ dye was added to cell cultures and the green fluorescence signal, which is produced by the binding interaction with dead cells' DNA, was measured following the manufacturer's instruction using a 2300 EnSpire™ multilable reader (PerkinElmer)

2.8 Immunoblotting

Cell cultures were exposed to OLA, OXA or their combination for 18h (detection of γH2AX) or 48 h (apoptosis evaluation). Cells were then harvested and lysed in 60 µl RIPA buffer containing protease and phosphatase inhibitors (Sigma Aldrich). The homogenates were left 20 minutes on ice and then centrifuged 15 min at 10000g. 30 µg protein of the supernatants (measured according to Bradford) was loaded into 4-12% polyacrylamide gel for electrophoresis and run at 170V. The separated proteins were blotted on a low fluorescent PVDF membrane (GE Lifescience) using a standard apparatus for wet transfer with an electrical field of 70 mA for 16 h. The blotted membrane was blocked with 2.5% BSA and 2.5% Casein in TBS-TWEEN and probed with the primary antibody. The antibodies used were: γH2AX phosphorylated histone (Rabbit, cell signaling), BCL-2 (Mouse, Santa Cruz), BAX (Rabbit, Abcam), Actin (Rabbit, Sigma-Aldrich). Binding was revealed by a Cy5-labelled secondary antibody (anti rabbit-IgG, GE Lifescience; anti mouse-IgG, Jackson Immuno-Research). All incubation steps were performed according to the manufacturer's instructions. The signals of BCL-2 and BAX were developed sequentially on the same blot. Fluorescence of the blots was assayed with the Pharos FX Scanner (BioRad) at a resolution on 100 µm, using the Quantity One software (BioRad).

2.9 Assessment of cell death with vital dyes.

BxPC-3 and SW620 cells were grown on coverslips placed in a 6-multiwell plate (5-10 x 10^5 cells/well). After a 48-h treatment with combined OLA and OXA, wells were rapidly washed with PBS and filled with 500 µl of a PBS solution containing 4′,6-diamidino-2-phenylindole (DAPI, 4.6 µg/ml) and propidium iodide (PI, 50 µg/ml). After a 10-min incubation at room temperature under light-shielded condition, they were washed with PBS, fixed (10 min) with 10% neutral buffered formalin solution, and washed again to eliminate the fixative. Coverslips were then applied on glass slides using two drops of mounting media

(DABCO). Images were acquired on a Nikon fluorescent microscope equipped with filters for DAPI and PI.

2.10 Statistical analysis

All data were analyzed by using the Prism 5 GraphPad software. All assays were repeated at least two times and in each experiment triplicate samples per treatment group were used. Results are expressed as mean ± SE of repeated experiments; p values < 0.05 were considered statistically significant.

3. Results

3.1 Metabolic characterization of SW620 and BxPC-3 cultures

To characterize the metabolic asset of SW620 and BxPC-3 cells we evaluated the expression of the two LDH isoforms (LDH-A and -B); furthermore, we assessed the levels of lactate and ATP in cultures exposed to oxamate (OXA), a well-studied LDH inhibitor, active in the millimolar range. Results are shown in Fig. 1.

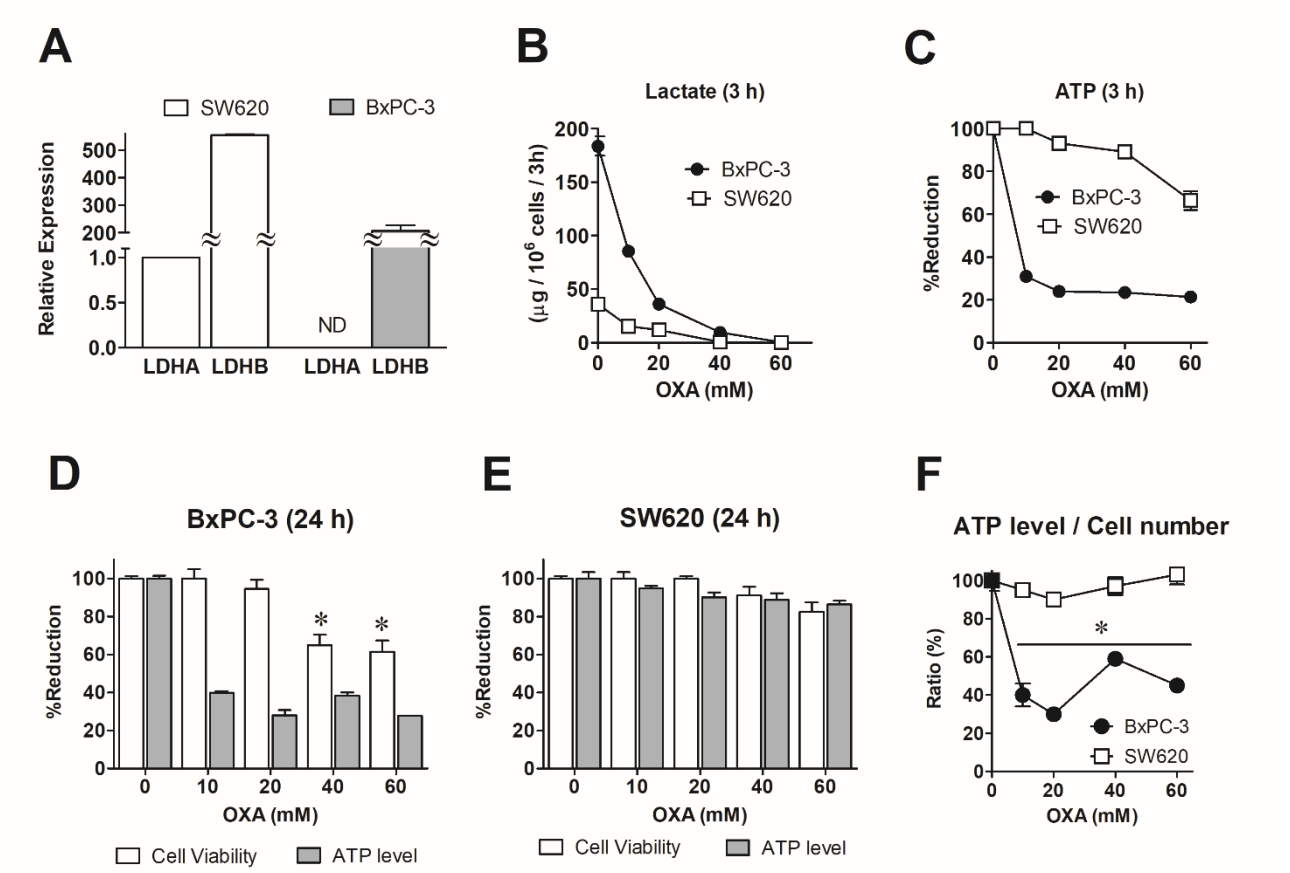

Figure 1 - Metabolic characterization of cell cultures

(A) Evaluation of LDH-A and -B expression by real-time PCR. ND, not detectable. (B) Lactate and (C) ATP levels measured in BxPC-3 and SW620 cells exposed to OXA. (D,E) Effect of OXA on the viability of the two cell cultures, assessed through the measure of ATP level or by evaluating cell number. In the case of BxPC-3 cells, the two procedures gave different results; when cell viability was assessed by evaluating cell number, no statistically significant effect appeared to be produced by 10 and 20 mM OXA at 24 h. Viability data were analyzed were analyzed by one-way ANOVA followed by Dunnet's post-test. *, $p < 0.01$ compared to control cultures. (F) Ratio ATP level / cell number, calculated from the results shown in (D,E). Data were analyzed one-way ANOVA followed by Dunnet's post-test. (*) $p < 0.01$ compared to control cultures. For further explanation, see text.

The bar graph in Fig. 1A shows the relative levels of LDH-A and -B measured in the two cultures, normalized on the LDH-A expression of SW620 cells. Both cultures showed a clear prevalence of the B isoform of the enzyme. Contrary to the current opinion linking LDH-A to actively glycolytic metabolism [13], BxPC-3 cultures, in which the -A isoform of the enzyme was undetectable, showed an energy metabolism highly dependent on glycolytic

reactions and resulted extremely susceptible to OXA (Fig. 1B,C). The rate of lactate production measured in these cells was 4-fold higher than that measured in SW620 cultures; moreover, their ATP content dropped to a very low level when exposed to OXA, given at a dose as low as 10 mM. The data of Fig. 1B,C also suggest that, opposite to BxPC-3 cultures, SW620 cells mainly base their energy metabolism on oxidative reactions, since they appeared to maintain not significantly modified ATP levels even in the presence of 40 mM OXA, a dose which almost completely abolished lactate production.

The two different metabolic assets of these cell cultures were also confirmed by studying the effect of OXA on cells viability, assessed after a 24 h treatment by using two different procedures: the Neutral Red assay (which gives an estimate of cell number) and the CellTiter-Glo Assay (which measures ATP levels). Results (Fig. 1D,E) showed that in SW620 cells the two procedures give superimposable results, and confirmed that energy metabolism and viability of these cells are unaffected by LDH inhibition, at 24 h. In these cultures, the ratio ATP / cell number was unchanged for all tested doses of OXA (Fig. 1F). When performed on BxPC-3 cultures, the same experiments showed that although LDH inhibition significantly impacted on the energy metabolism of these cells, no significantly reduction of viability was produced by 10-20 mM OXA. It is worth notice that although viable, these cultures showed ATP levels reduced up to 30% (Fig. 1D,F).

3.2 Study of homologous recombination in LDH-inhibited cells

Both cultures were exposed to OXA given for 16 h at a dose causing significant inhibition of LDH enzymatic activity (Fig. 1B) without affecting cell viability: 10-20 mM OXA was used for BxPC-3; 40 mM for SW620 cultures. To test HR function in OXA-exposed cultures, we applied the following procedures: a) we assessed the expression of genes involved in HR repair; b) evaluated plasmid recombination in transfected cells; c) estimated

the extent of DNA damage caused by olaparib (OLA); d) visualized nuclear localization of RAD51 induced by a DNA damaging agent.

The expression level of a panel of genes which are key drivers of HR repair [24] was assessed by real-time PCR: BRCA1 and -2; RAD51 and genes of the MRN complex (MRE11A; RAD50; NBN). Results are reported in Fig. 2A, B.

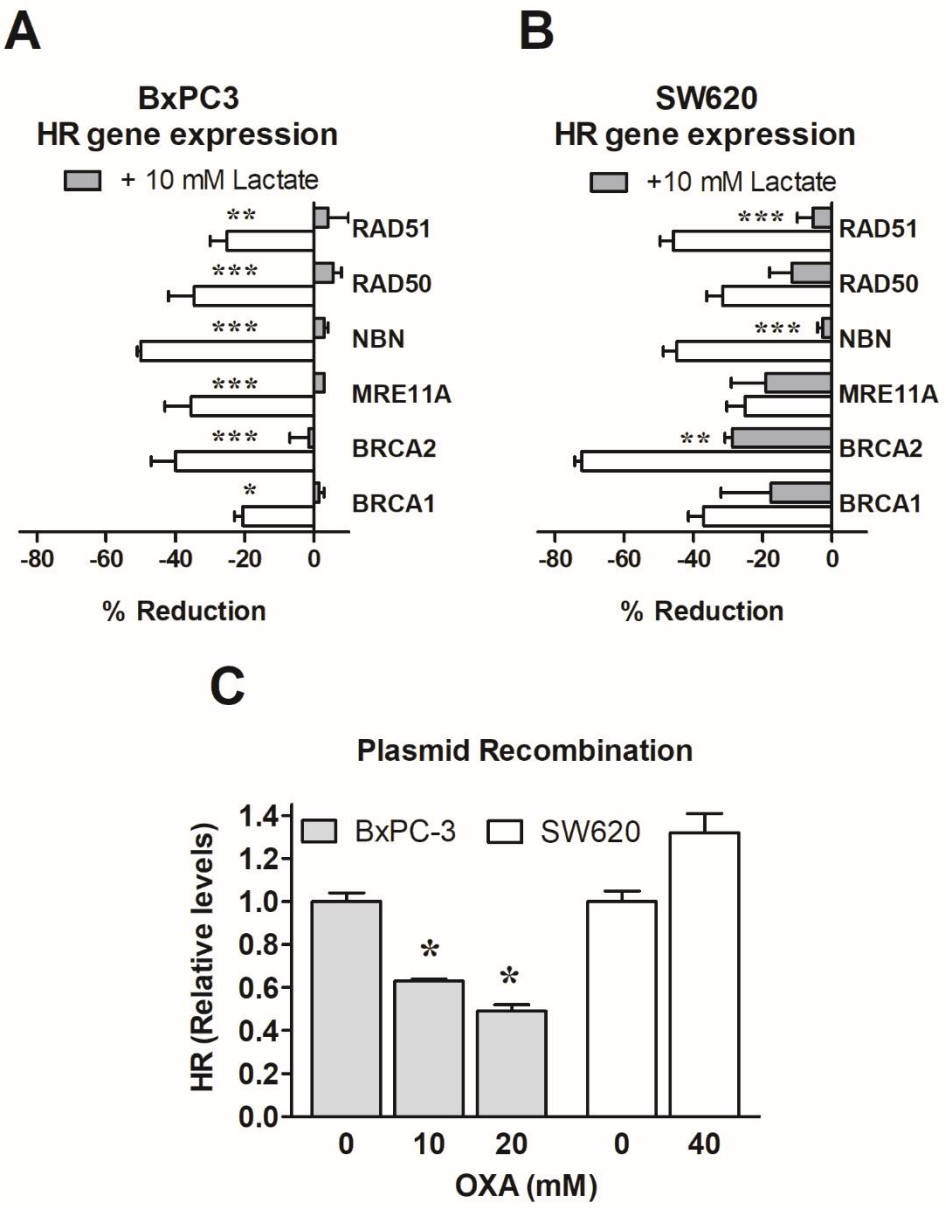

Figure 2 – Expression level of HR genes and plasmid recombination in LDH-inhibited cells.

A group of key genes involved in the HR pathway was examined by real-time PCR in BxPC-3 (A) and SW620 cultures (B) exposed for 16 h to OXA. Data were evaluated using one-way ANOVA followed by Dunnet's post-test. In BxPC-3 cells, a statistically significant reduced expression was found for all examined

genes, with the exception of BRCA1; p values ranged from <0.05 to <0.01. In the case of SW620 cells, a statistically significant difference compared to control cultures was observed for all genes, with p<0.01. The graphs also show the effect of lactate supplementation on gene expression (grey bars). In spite of their ATP-lowered content, BxPC-3 cells proved to be very responsive to this metabolite, which completely reversed all the OXA-driven effects. In SW620 cells lactate was able to significantly reverse the effects of LDH inhibition in 3 out of 6 genes. (*), p < 0.05; (**) < 0.01 (**); (***) < 0.001. (C) Episomal plasmid recombination assessed in the two cell lines by using a commercially available assay. For explanation, see text. In BxPC-3 cells, a statistically significant reduction was observed for both OXA doses, with p < 0.05 (*) (ANOVA).

Predictably, in ATP-depleted BxPC-3 cells the expression of all examined genes appeared significantly lowered, with a variation ranging from -22% (BRCA1) to -50% (NBN) (Fig. 2A). However, a statistically significant reduced expression of the same gene panel was also observed in SW620 cells, in which even higher effects were observed (-72% for BRCA2; -46% for RAD51) (Fig. 2B). In some experimental settings the product of LDH reaction (which in these cells was completely abolished by the used dose of OXA (Fig. 1B)) was found to impact on histone acetylation and gene expression [17]. For this reason and in search of a possible explanation to the result observed in SW620 cells, we exposed both cultures to the same OXA treatment supplemented with 10 mM lactate. In line with published data, lactate supplementation was found to significantly reverse most of the changes observed in SW620 cells (Fig. 2B). Unexpectedly, in spite of their ATP-lowered content BxPC-3 cells were more responsive to the effects of this metabolite (Fig. 2A).

Taken together, the results shown in Fig. 2A, B suggest that LDH activity could be involved in controlling the expression of a crucial group of genes involved in HR. Depending on the cell context, the role of this enzyme in maintaining energy balance can contribute in causing the downregulated gene expression; however, a major impact appears to derive from the non-metabolic functions of the LDH reaction product.

Fig. 2C shows the results obtained by applying to OXA-exposed cultures a commercially available assay specifically designed to study the co-transformation in

bacterial cells of two plasmids bearing homology sequences. The provided couple of plasmids can be also transfected into mammalian cells. In these cells, they recombinate in episomal form using the enzymatic machinery of the host and produce a real-time PCR detectable sequence. In line with the results of Fig. 2A, in BxPC-3 cells the obtained recombination product appeared to be significantly decreased. On the contrary, in SW620 cultures higher rates of plasmid recombination were detected. To explain this finding, we hypothesized that in these cultures alternative pathways of DNA recombination can take place when HR genes are down regulated. These pathways have also been described as more rapid and, consequently, more error prone, when compared to HR. Table 1 shows a list of genes involved in alternative recombination pathways, as recognized by [25]: classical non-homologous end joining (NHEJ) and alternative end joining (EJ). The expression of these genes was examined in both the OXA-treated cultures.

Table 1

Expression of genes involved in alternative pathways to homologous recombination repair. Changes observed in cells exposed to OXA.

Gene	Protein	DDR Pathway	% Variation in BxPC3 cells	% Variation in SW620 cells
DCLRE1C	Artemis	Classical NHEJ	ND*	ND
LIG4	Ligase 4		- 21 ± 9	ND
PRKDC	DNAPKcs		ND	ND
XRCC4	XRCC4		- 38 ± 7	- 34 ± 3
XRCC5	Ku80		- 46 ± 6	ND
XRCC6	Ku70		- 48 ± 8	ND
LIG1	Ligase 1	Alternative EJ	ND	- 38 ± 4
PARP1	PARP		-30 ± 2	ND
WRN	Werner helicase		ND	ND
XRCC1	XRCC1		ND	ND

***** ND, not detected. Only changes exceeding 20% have been considered.

Predictably, in ATP depleted BxPC-3 cells 5 out of 10 examined genes involved in NHEJ and/or alternative EJ were found to be downregulated. On the contrary, in SW620 cells a reduced expression was detected only in 2 genes, suggesting that in these cultures the alternative pathways could work and their prompt activity should allow rapid recombination events.

The results of the third applied assay are reported in Fig. 3.

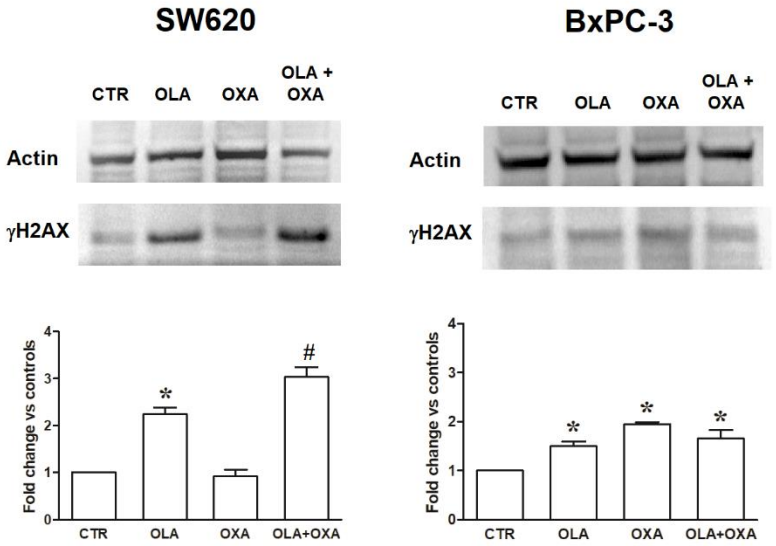

Figure 3 – Evaluation of DNA damage

DNA damage was assessed by an immunoblotting evaluation of H2AX histone phosphorylation (γH2AX). The experiment was performed in both cell cultures exposed for 16 h to OXA and 10 μM OLA, administered separately or in association. 10 and 40 mM OXA were used in BxPC-3 and SW620 cells, respectively. The bar graphs show a densitometric estimation of γH2AX bands, normalized on Actin levels. In the case of SW620 cells, OLA was found to significantly increase γH2AX level; the extent of DNA damage was further raised by the association OXA/OLA. In BxPC-3 cells a slight, but statistically significant increased level of γH2AX was observed in all treated samples; however, in these cells OXA did not caused increased DNA damage in OLA-exposed cultures. *, $p < 0.05$, compared to control cells. #, $p < 0.05$, compared to OLA treated cells (one-way ANOVA and Bonferroni's post-test).

For this experiment, cells were exposed for 16 h to OXA administered singularly or in association with OLA (10 μM) a PARP inhibitor which affects the base-excision repair mechanism [26]. This OLA dose was chosen on the basis of previous results, obtained by studying the association of OLA with different inhibitors of HR [27-29]. As well documented, in conditions of compromised HR repair (e.g. in BRCA1/2 defective cancer cells) PARP inhibition results in increased DNA damage signatures [20], which can be evaluated by assessing γH2AX levels [30]. This effect was entirely reproduced in SW620 cells exposed to the association of the two compounds. In these cultures, OLA caused enhanced γH2AX

levels, but the simultaneous exposure to OXA was found to significantly increase the effects of PARP inhibition, giving a proof compromised HR in LDH-inhibited cells.

On the contrary, and in spite of the results obtained in the two previous assays (Fig. 2A, 2C), LDH inhibition did not appear to induce significantly increased DNA damage in OLA-exposed BxPC-3 cells. In our opinion, this result can be easily explained considering that ATP deprivation of LDH-inhibited BxPC-3 cells is expected to impact on phosphorylation-mediated signaling and to reduce cell competence in managing DNA damage.

A further proof of compromised HR in LDH-inhibited cells was obtained by studying RAD51 nuclear translocation following a short exposure to cisplatin (CPL), a chemotherapeutic agent causing direct DNA damage [31]. BRCA2-mediated translocation of RAD51 in cell nuclei is one of the earliest events at the onset of HR repair [32]; the nuclear localization of RAD51 can be evidenced by an immunofluorescence staining of this protein in CPL treated cells. Results are shown in Figure 4.

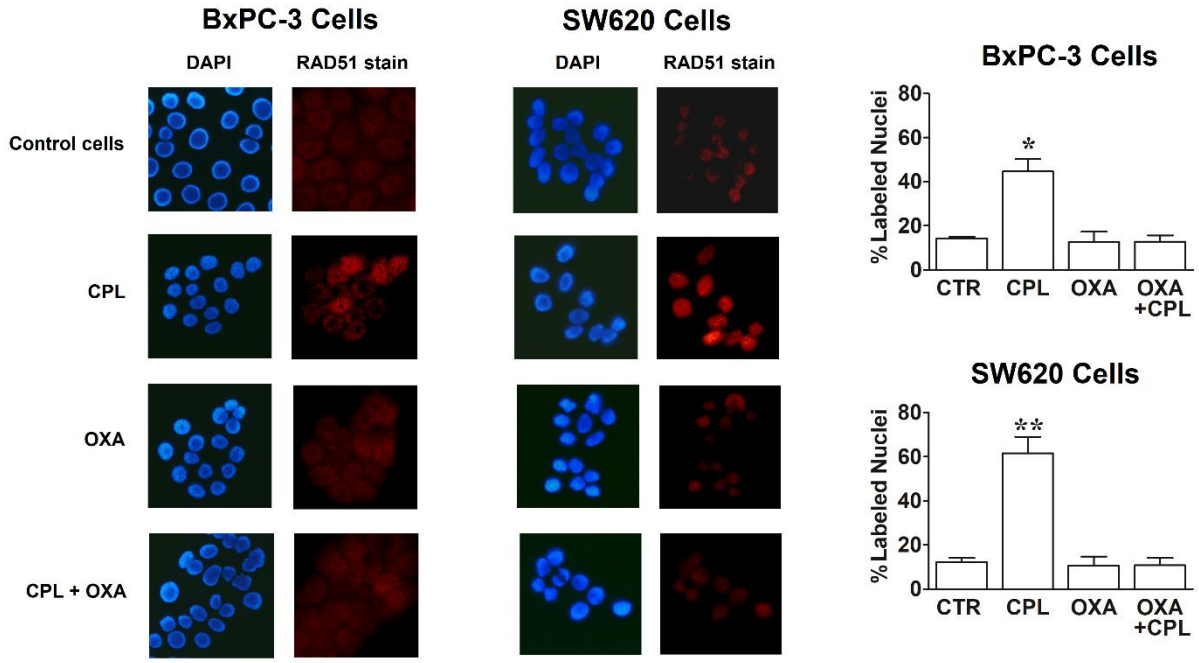

Figure 4 – RAD51 Immunostaining in cell nuclei after cisplatin treatment

Cell cultures were probed with 50 μM CPL for 1.5 h and maintained in the presence of OXA for 24 h. The detailed procedure of the experiment is described in Materials and Methods, paragraph 2.5. The data reported in the bar graphs were statistically evaluated by one-way ANOVA followed by Dunnet's post-test. Asterisks indicate a significant difference compared to untreated cells (CTR), with $p < 0.05$ (*) and $p < 0.01$ (**).

In this experiment, CPL was found to significantly increase RAD51 immunolabeling in the nuclei of both BxPC-3 and SW620 cultures, with a p value < 0.05 and 0.01, respectively. When administered to untreated cells, OXA did not modify the nuclear immunolabeling of RAD51; on the contrary, when administered to CPL-probed cells, the LDH inhibitor appeared to reduce RAD51 immunolabeling in nuclei to a level not dissimilar from that of untreated cells.

Taking these data together, in both BxPC-3 and SW620 cultures three of the four applied procedures to evidence inhibited HR after LDH inhibition gave coherent results. In both cultures, we observed a single inconsistency: in OLA-exposed BxPC-3 cultures, OXA treatment did not result in increased DNA damage; in OXA-treated SW620 cells, plasmid recombination was found to proceed at even higher rates. Since both these discrepancies

can be easily explained, the obtained results overall suggest that LDH inhibition reduce operative HR in both the used cell cultures, independently of their different metabolic asset.

3.3 Combination experiments with OXA and OLA

Recently, dampening HR through the use of small molecules inhibitors of the RAD51/BRCA2 complex has been proposed as a way to broaden the use of PARP inhibitors in anticancer therapy [27-29]. The rationale underlying this therapeutic approach is based on clinical studies reporting high therapeutic power for OLA (and other PARP inhibitors) in cancer contexts characterized by loss of BRCA1/2 function, which prevents HR [20]. These data can be explained considering that PARP function is crucial to mend single strand breaks in DNA and that when this function is not operative, DNA repair via HR becomes crucial for cell survival [20].

Figure 5 shows combination experiments with OXA and OLA, aimed at assessing cell viability and death caused by the compounds' association. The obtained data were statistically evaluated by two-way ANOVA using the OLA doses and OXA supplementation as variables.

In BxPC-3 cells (Fig. 5A), the potency of the compounds' association increased in parallel with the doses of OLA and OXA, and this effect was observed in the study of both cell viability and death. In both experiments, the statistical evaluation showed a strongly significant interaction between the two compounds, with $p < 0.0001$. Interestingly, the heavily lethal effects observed in these cells at 48 h cannot be simply ascribed to the impaired energy metabolism caused by LDH inhibition, since they appeared only in cultures treated with the compounds' association.

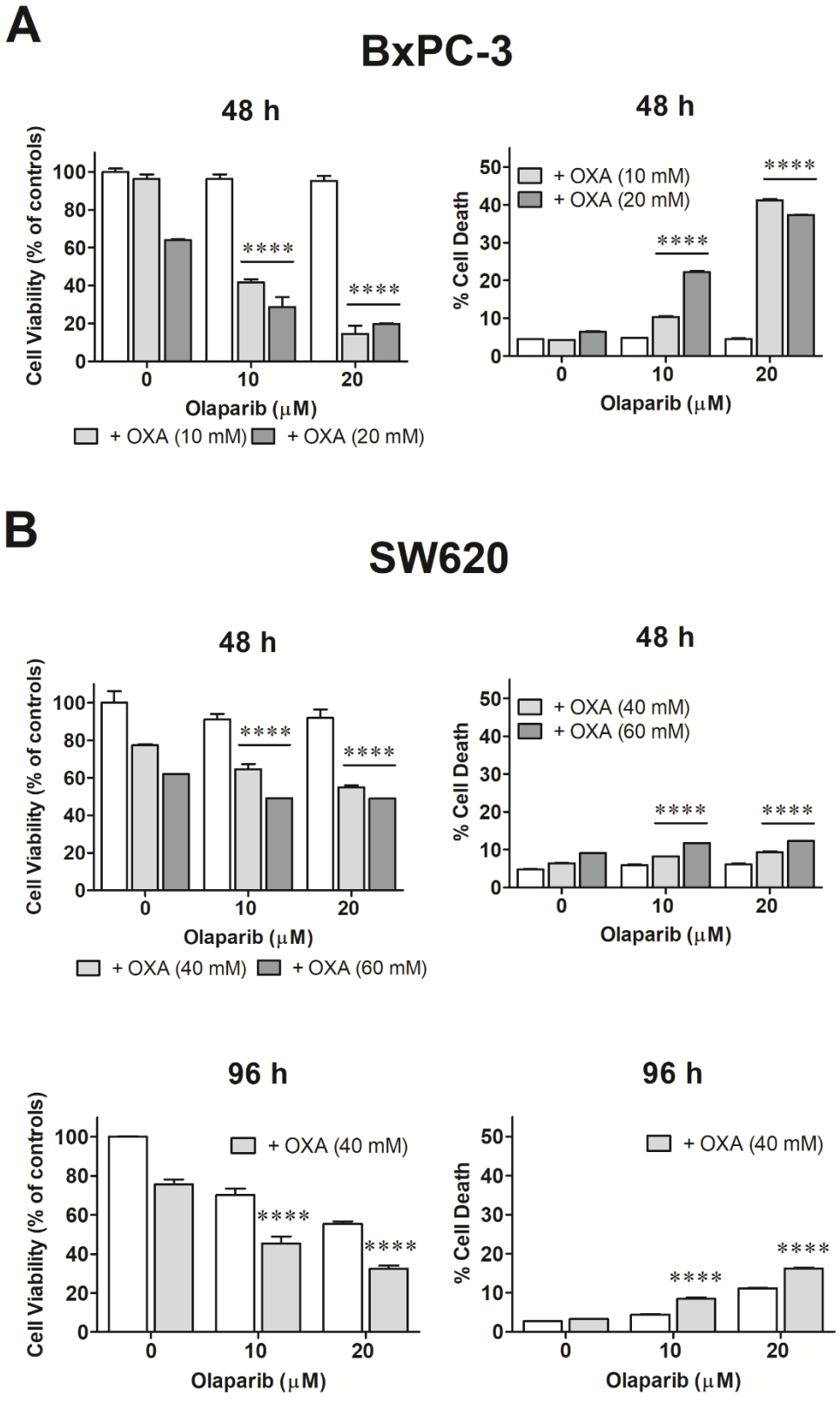

Figure 5 – Cell viability and death in combination experiments with OXA and OLA

Cell viability was studied by applying the Neutral Red assay in BxPC-3 (A) and in SW620 (B) cultures treated for the indicated time with OXA and OLA, administered singularly or in combination. Cell death was assessed by using the CellTox™ Green Cytotoxicity Assay (Promega), following the instruction of the

manufacturer. Data were statistically analyzed by applying the two-way ANOVA, using OLA and OXA supplementation as variables. ****, $p < 0.0001$, when compared to OLA administered as a single treatment (Bonferroni's post-test). The viability data reported in (A) and (B) were also used for an estimation of the C.I. of the OXA/OLA association, using the procedure described in [34]. A detailed explanation of the obtained results is given in the text.

In studying cell viability of the SW620 cultures (Fig. 5B), a statistically significant effect caused by OXA and OLA was observed, both at 48 and 96 h, with p values ranging from 0.0002 to < 0.0001. However, in this case the statistical analysis indicated no interaction between the two compounds, suggesting that, although statistically significant, the effect of OXA supplementation is similar for both the tested doses of OLA. Although in SW620 cultures the evidence of cell death caused by the association OLA/OXA was quite lower than that observed in BxPC-3 cells, the interaction between the two compounds on this parameter resulted statistically significant, with $p = 0.039$ at 48 h and $p < 0.0001$ at 96 h.

These results suggest that the increased potency of the compounds' association is mainly evidenced when considering its lethal effects, even though the entity of these effects can variate depending on the cell context. Notably, previous works showed the induction of alternative recombination pathways to be a crucial factor driving lethality in cells with inhibited HR and PARP function [33] and, as described above, in OXA-treated SW620 cells these pathways seem to be operative.

The potency of the OXA/OLA association was also evaluated by applying to the data of cell viability shown in Fig. 6 the procedure developed by Dos Santos Ferreira et al. [34] to assess the combination index (CI) between an enzyme inhibitor and antineoplastic agents. This calculation procedure (see Section 2.6) is applied to the fraction number of cells surviving the treatment and was already used to evaluate the potency of the association OLA / HR inhibitors [27-29]. According to [34], a CI ranging from 0.8 to 1.2 denotes an additive effect; synergism is indicated by a result <0.8; antagonism by a result >1.2. When

applied to the overall viability data obtained in BxPC-3 cells, this procedure returned a CI = 0.35, with a 95% confidence interval ranging from 0.12 to 0.58, clearly indicating for these cells the occurrence of synergism between the two compounds. In the case of SW620 cultures, a CI = 0.84 was measured, with a 95% confidence interval ranging from 0.77 to 0.91. Therefore, in this case the interaction between OXA and OLA appeared to be characterized by additive effects. Taken together, the results obtained by applying the calculation method suggested in [34] are in total agreement with the indications given by the two-way ANOVA test.

The experiments shown in Fig. 6 were aimed at better defining the cell death pattern observed in the two cell cultures.

In the experiments of Fig. 6A, the two cell cultures were exposed to the OLA/OXA association for 48 h and then treated with vital dyes (DAPI and PI) without a fixation step in paraformaldehyde. The simultaneous use of these two dyes can demonstrate cell death, also giving indication on the death pattern [35]. DAPI is cell-permeable and evidences nuclear morphology; healthy cells appear to display normal nuclear morphology in the absence of PI staining, since this dye is not cell-permeable. Cells undergoing apoptosis display nuclear condensation, which is indicated by increased DAPI staining. PI staining indicates compromised membrane integrity, which characterizes necrotic cells and late-apoptotic cells maintained in culture. The DAPI/PI staining procedure confirmed the massive death of BxPC-3 cells already observed at 48 h in the experiments of Fig. 5A. The bright PI staining of these cultures suggest loss of membrane integrity, as can be expected in cells with compromised energy metabolism.

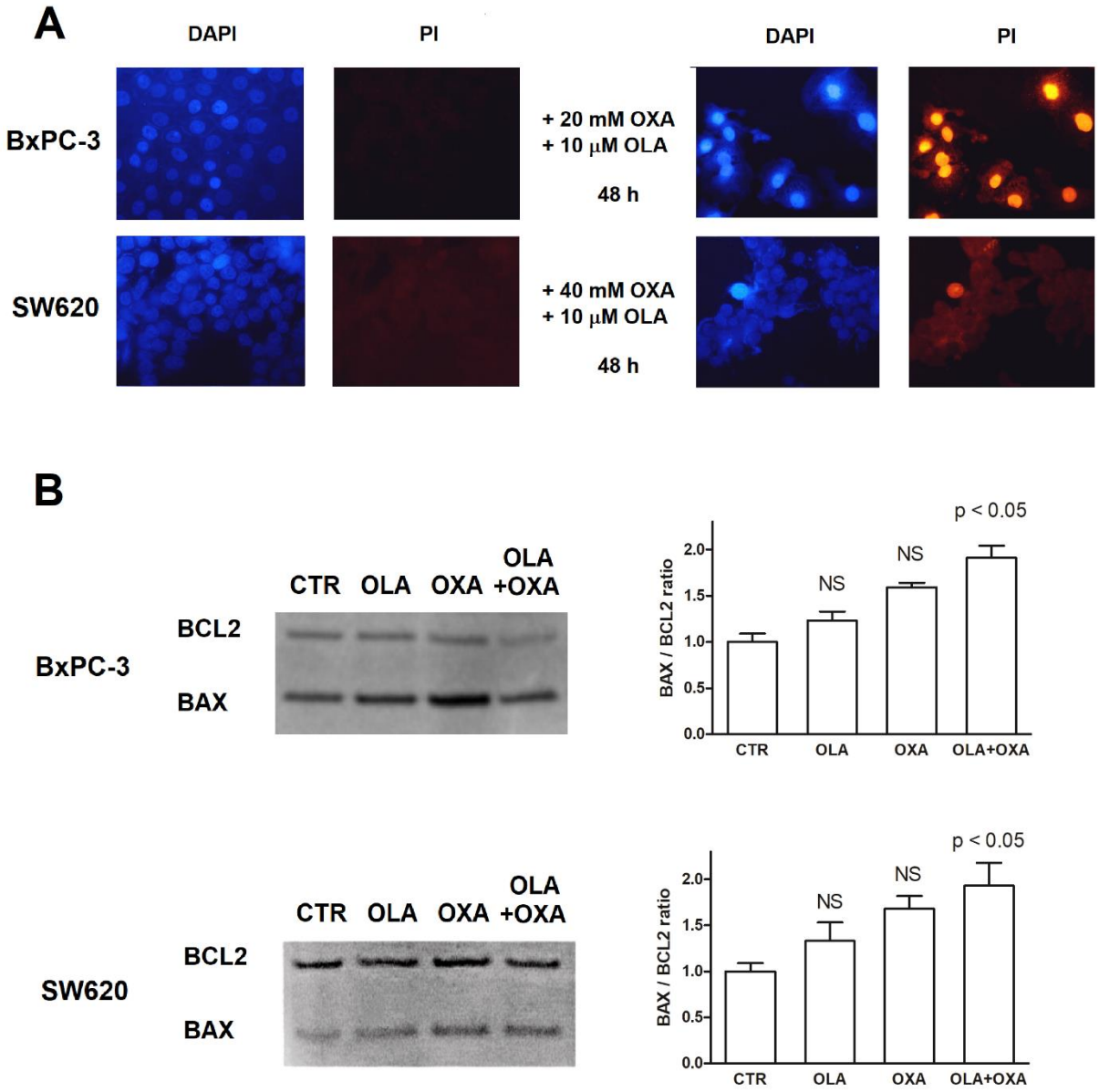

Figure 6 – Cell death in cultures treated with the combination OXA/OLA

(A) Assessment of cell death with vital dyes. In BxPC-3 cells death appeared to be sharply evident. The observed staining pattern is compatible with apoptosis (increased DAPI staining suggesting nuclear condensation) followed by damaging of membranes (deep PI staining). In SW620 cultures PI staining pattern appeared pale and limited to some areas of the microscope slide. For this reason, an additional assay was applied to these cells. (B) Assessment of apoptosis at the molecular level, through the immunoblotting evaluation of BAX/BCL2 ratio. As shown in the bar graph, only cultures treated with the compounds' association showed a statistically significant difference in their BAX/BCL2 ratio when compared with untreated cells (ANOVA) NS, not significant.

In agreement with the data of Fig. 5B, in treated SW620 cultures a low level of cell death was observed at 48 h. For this reason, cell death was further investigated by an immunoblotting evaluation of the BAX/BCL2 ratio, which was performed in both cell lines. As shown in Fig. 6B, although BxPC-3 and SW620 cells appeared to express different BAX and BCL2 levels, the densitometric calculation of the ratio between the two proteins showed superimposable changes in response to the applied treatments. In both cultures, apoptosis appeared to be significantly increased (compared to control cells) only as a result of the combined OLA/OXA treatment. The findings reported in Fig. 6B suggested that the molecular signatures of apoptosis were evident in both cell cultures at a very similar level; furthermore, they indirectly confirmed that the reduced ATP availability of OXA-exposed BxPC-3 cells can be the key factor in generating the membrane damage and the consequent heavy lethality observed in these cultures (Fig. 5B, 6A).

4. Discussion

Poor drug response is a major hitch limiting the success of anticancer therapy. This feature was found to be correlated with cell metabolic asset [8], but the role of LDH in this phenomenon was never extensively studied, although, as stated in the Introduction, this enzyme is a major player in cancer cell metabolism [10]. The data of our preliminary investigation suggest an LDH-mediated control on HR, the most critical DDR pathway for restoring chromosome integrity and, hence, potentially affecting cell response to chemotherapeutic agents. Our results indicate that this control could be exerted by simply assuring the adequate energy supply needed to the DDR and/or by regulating the expression level of genes involved in DNA repair. Although preliminary, they highlight a complex relationship between metabolic reactions and the control of DNA integrity.

Furthermore, they offer a mechanistic explanation to several published reports showing increased cell response to antineoplastic agents after LDH inhibition or knockdown [36-39].

In latest years, in the attempt of developing innovative anticancer strategies, treatments with small molecules able to hinder DNA repair have been proposed [40]. The rationale underlying this therapeutic approach lies in the genetic instability of cancer cells, which makes them more dependent on DNA repair mechanisms, compared to healthy cells. PARP inhibitors (e.g. OLA) are a well-known example of antineoplastic drugs targeting the DDR [26]. However, clinical experience with these compounds showed successful therapeutic results only on cancer forms characterized by HR deficiency [19,20], which cannot compensate for the inhibited PARP function. To broaden the use of PARP inhibitors, the association of OLA with conventionally used chemotherapeutics was also proposed [41], with the aim to obtain enhanced therapeutic power. Furthermore, the effect of this drug was tested in cancer contexts characterized by different DNA repair deficiencies, such as colon cancer with microsatellite instability [42]. However, these approaches were often found to produce increased systemic toxicity [41,42]; in addition, the potential increased risk of incurring in secondary malignancies, after the successful control of the primary tumor should be considered [43]. The findings described in this paper suggest a possible use of LDH inhibitors to extend the use of OLA to HR proficient tumor forms. Recently, the first LDH inhibitor potentially active *in vivo* has been identified [12]. In the used animal model, the only observed toxic effect that could potentially narrow the therapeutic window of this novel compound was found to be hemolysis, presumably linked to the metabolic inhibition of red blood cells. Taken together, these data suggest a combination of OLA with LDH inhibitors as a worthwhile therapeutic attempt to dampen the proliferative potential of cancer cells with tolerable side effects on normal tissues.

Funding

This work was supported by Cornelia and Roberto Pallotti's Legacy for Cancer Research, Associazione Italiana per la Ricerca sul Cancro AIRC (Progetto IG 2018, id 21386), and by University of Bologna (RFO funds).

Conflict of Interest Statement

The authors declare that there are no conflicts of interest.

References

[1] T.N. Seyfried, R.E. Flores, A.M. Poff, D.P. D'Agostino, Cancer as a metabolic disease: implication for novel therapeutics, Carcinogenesis 35 (2014) 515-527.

[2] G.L. Semenza, Tumor metabolism: cancer cells give and take lactate, J. Clin. Invest. 118 (2008) 3835-3837.

[3] S.Y. Lunt, M.G. Vander Heiden, Aerobic glycolysis: meeting the metabolic requirements of cell proliferation, Annu. Rev. Cell. Dev. Biol. 27 (2011) 441-464.

[4] J. Yang, B. Ren, G. Yang, H. Wang, G. Chen, L. You, T. Zhang, Y. Zhao, The enhancement of glycolysis regulates pancreatic cancer metastasis, Cell. Mol. Life Sci. 77 (2020) 305-321.

[5] K. Matsuura, K. Canfield, W. Feng, M. Kurokawa, Metabolic regulation of apoptosis in cancer, Int. Rev. Cell. Mol. Biol. 327 (2016) 43–87.

[6] A. Krüger, M. Ralser, ATM is a redox sensor linking genome stability and carbon metabolism, Sci. Signal. 4 (2011) pe17.

[7] A.N. Bhatt, A. Chauhan, S. Khanna, Y. Rai, S. Singh, R. Soni, N. Kalra, B.S. Dwarakanath, Transient elevation of glycolysis confers radio-resistance by facilitating DNA repair in cells, BMC Cancer 15 (2015) 335.

[8] M.A.T. vanVugt, Shutting down the power supply for DNA repair in cancer cells, J. Cell Biol. 216 (2017) 295-297.

[9] R.A. Gatenby, R.J. Gillies, Why do cancers have high aerobic glycolysis?, Nat. Rev. Cancer 4 (2004) 891-899.

[10] L. Fiume, M. Manerba, M. Vettraino, G. Di Stefano, Inhibition of lactate dehydrogenase activity as an approach to cancer therapy, Future Med. Chem. 6 (2014) 429-445.

[11] S.L. Zhang, Y. He, K.Y. Tam, Targeting cancer metabolism to develop human lactate dehydrogenase (hLDH)5 inhibitors, Drug Discov. Today. 23 (2018) 1407–1415.

[12] C. Yeung, A.E. Gibson, S.H. Issaq, N. Oshima, J.T. Baumgart, L.D. Edessa, G. Rai, D.J. Urban, M.S. Johnson, G.A. Benavides, G.L. Squadrito, M.E. Yohe, H. Lei, S. Eldridge, J. Hamre III, T. Dowdy, V. Ruiz-Rodado, A. Lita, A. Mendoza, J.F. Shern, M. Larion, L.J. Helman, G.M. Stott, M.C. Krishna, M.D. Hall, V. Darley-Usmar, L.M. Neckers, C. M. Heske, Targeting glycolysis through inhibition of lactate dehydrogenase impairs tumor growth in preclinical models of Ewing sarcoma, Cancer Res. 79 (2019) 5060-5073.

[13] H. Shim, C. Dolde, B.C. Lewis, C.S. Wu, G. Dang, R.A. Jungmann, R. Dalla Favera, C.V. Dang, c-Myc transactivation of LDH-A: Implications for tumor metabolism and growth, PNAS 94 (1997) 6658-6663.

[14] S.L. Sheng, J.J. Liu, Y.H. Dai, X.G. Sun, X.P. Xiong, G. Huang, Knockdown of lactate dehydrogenase A suppresses tumor growth and metastasis of human hepatocellular carcinoma, FEBS J. 279 (2012) 3898-3910.

[15] A.E. Boukouris, S.D. Zervopoulos, E.D. Michelakis, Metabolic enzymes moonlighting in the nucleus: metabolic regulation of gene transcription, Trends Biochem. Sci. 41 (2016) 712-730.

[16] R.P. Dai, F.X. Yu, S.R. Goh, H.W. Chng, Y.L. Tan, J.L. Fu, L. Zheng, Y. Luo, Histone 2B (H2B) expression is confined to a proper NAD+/NADH redox status, J. Biol. Chem. 283 (2008) 26894-26901.

[17] W. Wagner, W.M. Ciszewski, K.D. Kania, L- and D-lactate enhance DNA repair and modulate the resistance of cervical carcinoma cells to anticancer drugs via histone deacetylase inhibition and hydroxycarboxylic acid receptor 1 activation, Cell Comm. Signaling 13 (2015) 36.

[18] W. Wagner, K.D. Kania, W.M. Ciszewski, Stimulation of lactate receptor (HCAR1) affects cellular DNA repair capacity, DNA Repair (Amst) 52 (2017) 49-58.

[19] K.P. Pennington, T. Walsh, M.I. Harrell, M. K. Lee, C.C. Pennil, M.H. Rendi, A. Thornton, B.M. Norquist, S. Casadei, A.S. Nord, K.J. Agnew, C.C. Pritchard, S. Scroggins, R.L. Garcia, M.C. King, E.M. Swisher, Germline and somatic mutations in homologous recombination genes predict platinum response and survival in ovarian, fallopian tube, and peritoneal carcinomas, Clin. Cancer Res. 20 (2014) 764-775.

[20] A.D. D'Andrea, Mechanisms of PARP inhibitor sensitivity and resistance, DNA Repair 71 (2018) 172-176.

[21] A. Ward, K.K. Khanna, A.P. Wiegmans, Targeting homologous recombination, new pre-clinical and clinical therapeutic combinations inhibiting RAD51, Cancer Treat. Rev. 41 (2015) 35–45.

[22] J. Papacostantinou, S.P. Colowick, The role of glycolysis in the growth of tumor cells. I. Effects of oxamic acid on the metabolism of Ehrlich tumor cells in vitro, J. Biol. Chem. 236 (1961) 278-284.

[23] F. Farabegoli, M. Vettraino, M. Manerba, L. Fiume, M. Roberti, G. Di Stefano, Galloflavin, a new lactate dehydrogenase inhibitor, induces the death of human breast

cancer cells with different glycolytic attitude by affecting distinct signaling pathways, Eur. J. Pharm. Sci. 47 (2012) 729-738.

[24] M. Krajewska, R.S.N. Fehrmann, E.G.E. deVriesand, M.A.T.M. vanVugt, Regulators of homologous recombination repair as novel targets for cancer treatment, Front. Genet. 9 (2015) 96.

[25] G. Iliakis, T. Murmann, A. Soni, Alternative end-joining repair pathways are the ultimate backup for abrogated classical non-homologous end-joining and homologous recombination repair: Implications for the formation of chromosome translocations, Mutation Research 793 (2015) 166-175.

[26] J. Mateo, C.J. Lord, V. Serra, A. Tutt, J. Balmaña, M. Castroviejo-Bermejo, C. Cruz, A. Oaknin, S.B. Kaye, J.S. de Bono, A decade of clinical development of PARP inhibitors in perspective, Ann. Oncol. 30 (2019) 1437-1447.

[27] F. Falchi, E. Giacomini, T. Masini, N. Boutard, L. Di Ianni, M. Manerba, F. Farabegoli, L. Rossini, J. Robertson, S. Minucci, I. Pallavicini, G. Di Stefano, M. Roberti, R. Pellicciari, A Cavalli, Synthetic lethality triggered by combining olaparib with BRCA2-Rad51 disruptors, ACS Chem. Biol. 12 (2017) 2491-2497.

[28] M. Roberti, F. Schipani, G. Bagnolini, D. Milano, E. Giacomini, F. Falchi, A. Balboni, M. Manerba, F. Farabegoli, F. De Franco, J. Robertson, S. Minucci, I. Pallavicini, G. Di Stefano, S. Girotto, R. Pellicciari, A. Cavalli, Rad51/BRCA2 disruptors inhibit homologous recombination and synergize with olaparib in pancreatic cancer cells, Eur. J. Med. Chem. 165 (2019) 80-92.

[29] G. Bagnolini, D. Milano, M. Manerba, F. Schipani, J.A. Ortega, D. Gioia, F. Falchi, A. Balboni, F. Farabegoli, F. De Franco, J. Robertson, R. Pellicciari, I. Pallavicini, S. Peri, S. Minucci, S. Girotto, G. Di Stefano, M. Roberti, A. Cavalli, Synthetic lethality in pancreatic cancer: discovery of a new RAD51-BRCA2 small molecule disruptor that

inhibits homologous recombination and synergizes with Olaparib, J. Med. Chem 63 (2020) 2588-2619.

[30] A. Sharma, K. Singh, A. Almasan, Histone H2AX phosphorylation: a marker for DNA damage, Methods Mol. Biol. 920 (2012) 613-626.

[31] A. Basu, S. Krishnamurthy, Cellular responses to cisplatin-induced DNA damage, J. Nucleic Acids 2010 (2010) pii 201367.

[32] A.A. Davies, J.Y. Masson, M.J. McIlwraith, A.Z. Stasiak, A. Stasiak, A.R. Venkitaraman, S.C. West, Role of BRCA2 in control of the RAD51 recombination and DNA repair protein, Mol. Cell 7 (2001) 273−282.

[33] A.G. Patela, J.N. Sarkariab, S.H. Kaufmann, Nonhomologous end joining drives poly(ADP-ribose) polymerase (PARP) inhibitor lethality in homologous recombination-deficient cells, PNAS 108 (2011) 3406-3411.

[34] A.C. Dos Santos Ferreira, R.A. Fernandes, J.K. Kwee, C.E. Klumb, Histone deacetylase inhibitor potentiates chemotherapy-induced apoptosis through Bim upregulation in Burkitt's lymphoma cells, J. Cancer Res. Clin. Oncol. 138 (2012) 317-325.

[35] B.S. Cummings, L.P. Wills, R.G. Schnellmann, Measurement of cell death in mammalian cells, Curr. Protoc. Pharmacol. (2012) 1-30 (Chapter 12, Unit 12.8).

[36] M. Zhou, Y. Zhao, Y. Ding, H. Liu, Z. Liu, O. Fodstad, A.I. Riker, S. Kamarajugadda, J. Lu, L.B. Owen, S.P. Ledoux, M. Tan, Warburg effect in chemosensitivity: targeting lactate dehydrogenase-A re-sensitizes taxol-resistant cancer cells to taxol, Mol. Cancer 9 (2010) 33.

[37] Y. Zhao, H. Liu, Z. Liu, Y. Ding, S.P. Ledoux, G.L. Wilson, R. Voellmy, Y. Lin, W. Lin, R. Nahta, B. Liu, O. Fodstad, J. Chen, Y. Wu, J.E. Price, M. Tan, Overcoming

trastuzumab resistance in breast cancer by targeting dysregulated glucose metabolism, Cancer Res. 71 (2011) 4585-4597.

[38] M. Manerba, L. Di Ianni, L. Fiume, M. Roberti, M. Recanatini, G. Di Stefano, Lactate dehydrogenase inhibitors sensitize lymphoma cells to cisplatin without enhancing the drug effects on immortalized normal lymphocytes, Eur. J. Pharm. Sci. 74 (2015) 95-102.

[39] X. Zhai, Y. Yang, J. Wan, R. Zhu, Y. Wu, Inhibition of LDH-A by oxamate induces G2/M arrest, apoptosis and increases radiosensitivity in nasopharyngeal carcinoma cells, Oncol. Rep. 30 (2013) 2983-2991.

[40] J.F.S. Carvalho, R. Kanaar, Targeting homologous recombination-mediated DNA repair in cancer, Expert Opin. Ther. Targets 18 (2014) 427-58.

[41] M. Yarchoan, M.C. Myzak, B.A. Johnson 3rd, A. De Jesus-Acosta, D.T. Le, E.M. Jaffee, N.S. Azad, R.C. Donehower, L. Zheng, P.E. Oberstein, R.L. Fine, D.A. Laheru, M. Goggins, Olaparib in combination with irinotecan, cisplatin, and mitomycin C in patients with advanced pancreatic cancer, Oncotarget 8 (2017): 44073-44081.

[42] L. Leichman, S. Groshen, B.H. O'Neil, W. Messersmith, J. Berlin, E. Chan, C.G. Leichman, S.J. Cohen, D. Cohen, H.J. Lenz, P. Gold, B. Boman, A. Fielding, G. Locker, R.C. Cason, S R. Hamilton, H.S. Hochsterk, Phase II study of olaparib (AZD-2281) after standard systemic therapies for disseminated colorectal cancer, The Oncologist 21 (2016) 172-177.

[43] C.Y. Li, Inhibitors of DNA repair for cancer therapy, ready for prime time?, Transl. Cancer Res. 1 (2012) 4-5.

Supplementary Information

Table S1

List of primer sequences used for RT-PCR analysis.

Gene	Forward primer (5' – 3')	Reverse primer (5' – 3')
LDH-A	GACCTACGTGGCTTGGAAGA	TCCATACAGGCACACTGGAA
LDH-B	CCAACCCAGTGGACATTCTT	AAACACCTGCCACATTCACA
BRCA1	TATCCGCTGCTTTGTCCTCA	TGCAGGAAACCAGTCTCAGT
BRCA2	GAGAGTTCCCAGGCCAGTAC	ACTGGAAAGGTTAAGCGTCA
NBN (Nibrin or P95)	CCACCTCCAAAGACAACTGC	TCAGGACGGCAGGAAAGAAA
MRE11 (Double Strand Break Repair Nuclease)	TGTTGAGGTTGCCATCTTGA	TGATCAGTCAGTCAACTTTGGT
RAD50 (Double Strand Break Repair Protein)	CTGCTTGTTGAACAGGGTCG	CCAATTCTAGCTGTGTTGCCA
RAD51 (Recombinase)	CAAATGCAGATACTTCAGTGGAA	TCCAGCTTCTTCCAATTTCTTCA
DCLRE1C (DNA cross-link repair 1C or Artemis)	TTCTCCCTATCGAAGCGGTC	ATGAGTTCTTTCGAGGGGCA
LIG4 (DNA Ligase 4)	GGTCGTTTACTTGCTGTATGGT	TGCATATTTTGTGTTGAAGCCA
PRKDC (DNA-PK)	GAGCTCAACGTACATGAAGTCA	TGTGGATTCGAACAACAAGGAG
XRCC4 (X-ray repair cross complementing 4)	GCATTGTTGTCAGGAGCAGG	TGAAGGAACCAAGTCTGAATGAG
XRCC5 (X-ray repair cross complementing 5 or Ku80)	AGAATCCCCATTTGAACAAGCA	GAAAGGGGATTGTCAGTGCC
XRCC6 (X-ray repair cross complementing 6 or Ku70)	GGGCAAGATGAAGGCTATCG	GTTCCGGCTCCATCAAATCC
LIG1 (DNA Ligase 1)	CACCACTCCATTCCACTCCT	AGGGAGAATTCTGACGCCAA
PARP1	GCTATCATCAGACCCTCCCC	GGTGGAAATGCTTGACAACCT

(Poly(ADP-ribose) polymerase 1)		
WRN (Werner syndrome RecQ like helicase)	AGTTCTTGTCACGTCCTCTGG	GGTGCCTATTTAAGTTAATGTCTGC
XRCC1 (X-ray repair cross complementing 1)	TCCCAATGTCCACACTGTGT	TCAAGGCAGACACTTACCGA
CYP33A (Cyclophilin 33A)	GCTGCCTGTGCACTCATGAA	CAGTGCCATTGTGGTTTGTGA
GUSB (Glucuronidase Beta)	CTCATTTGGAATTTTGCCGATT	CCGAGTGAAGATCCCCTTTTTA
RPS13 (Ribosomal Protein S13)	CCCCACTTGGTTGAAGTTGA	ACACCATGTGAATCTCTCAGGA
TUBA (Tubulin Alpha)	TGGAACCCACAGTCATTGATGA	TGATCTCCTTGCCAATGGTGTA